A new method of charged particle identification based on frequency spectrum analysis*

Jin-Tao Zhu(朱金涛) Guo-Fu Liu(刘国福)[1)] Jun Yang(杨俊)
Xiao-Liang Luo(罗晓亮) Lei Zhang(张磊) Li-Feng Ji(季利锋)
College of Mechatronics and Automation, National University of Defense Technology, Changsha 410073, China

Abstract: A new frequency domain method for charged particle identification, called Frequency Ratio Analysis (FRA), is proposed by analyzing the frequency spectra of proton pulses and alpha pulses acquired from a totally depleted Si detector. Identification performance of the FRA method is evaluated and compared with two time domain methods, the current pulse amplitude method and the second moment method. The results show that the FRA method is not only feasible and effective but also superior to the two time domain methods, as it achieves an obvious increase in value of the figure-of-merit (FOM).

Keywords: charged particle, identification, frequency spectrum analysis

PACS: 29.30.Hs, 29.40.Mc, 28.41.Rc **DOI:** 10.1088/1674-1137/40/3/036202

1 Introduction

Charged particle identification, i.e., confirming the atomic number (Z) and mass number (A) of a charged particle, is essential in nuclear physics experiments and radiation detection. In the past, the ΔE-E telescope method or/and the time-of-flight (TOF) method were mainly used to identify the various species of charged particles. However, the ΔE-E telescope technique needs the particles to have enough energy to punch through the ΔE detector, and thus has a high identification threshold [1]. The TOF method, on the other hand, can only confirm the mass number A, so only when combined with another method, usually the ΔE-E telescope method, can it obtain the atomic number Z of the particles. In contrast to these two methods, the pulse shape analysis (PSA) method can achieve the detection of A and Z simultaneously by utilizing more particle information and has a relatively low identification threshold for only using one E detector [1–4]. The current pulse shapes acquired from the E detector, usually a totally depleted Si detector, are mainly determined by the plasma erosion effect and the charge carrier collection effect, both of which vary with particle species [5, 6]. For example, a heavier ion generates a longer duration but smaller amplitude in contrast to a lighter ion with the same energy [7]. By analyzing the differences of these current pulse shapes, different charged particles can be identified.

Since the PSA method was first proposed in 1963, it has drawn more and more attention and a wide variety of pulse features have been extracted to realize this method [8]. First the value at the specified time of the current pulse was used to identify charged particles and then the rise time of the pulse was applied in the discrimination of the proton and the alpha particles [9]. During the 1990s, G. Pausch et al. were very active in the charged particle identification field, first introducing the charge balance parameter method and the charge integration method that have been widely used in n/γ discrimination into PSA [7, 10–13]. Moreover, they built a semi-empirical model to simulate the current pulse in silicon detectors for heavy ions [11]. However, the methods mentioned above were mainly realized by analog electric circuits and by trial and error, which made them a little complex and inconvenient. With the development of digital techniques and the advantages of high speed sampling rate and large scale storage volume, a complete pulse waveform rather than the peak value of the pulse can be achieved, which broadens the imagination space when proposing new methods. In 2004, H. Hamrita et al. used the second moment of the current pulse to discriminate ^{12}C and ^{13}C with digital electric circuits [14]. In 2009, S. Barlini et al. then defined different moments of the pulse and chose two of them as characteristic parameters to identify heavy ions [1].

It is worthwhile to note that all the features extracted from the pulse waveform to realize the PSA method mentioned above stem from the analysis and calculation of

Received 6 May 2015, Revised 29 August 2015
∗ Supported by National Natural Science Foundation of China (11175254, 11375264)
1) E-mail: guofu.liu@nudt.edu.cn

the waveform data in the time domain, and none of the features come from the frequency domain. However, as an important tool for signal processing, frequency spectrum analysis methods, such as the Fourier transform and the wavelet transform, can reveal the essential characteristics of the analyzed waveform. In fact, some frequency domain methods have been applied in n/γ discrimination [15–18], all obtaining good discrimination performance. Therefore, we here introduce the frequency spectrum analysis method into the charged particle identification field by taking the identification of protons and alpha particles as an example. A new method called Frequency Ratio Analysis (FRA) is proposed by analyzing the differences between these two kinds of particles and by finding out their essential characteristics, and is evaluated by comparing with widely-used time domain methods.

This paper is organized as follows. In Section 2, the experimental setup and the energy calibration process are introduced. Section 3 illustrates the principle of the FRA method and its identification performance as well as its comparison with other methods. Finally, the conclusions arising from this research are stated in Section 4.

2 Experimental method

2.1 Experimental setup

The measurements were performed in the Institute of Nuclear Physics and Chemistry, the Chinese Academy of Engineering Physics. A schematic diagram of the experiment is sketched in Fig. 1. Two kinds of particles, alpha particles and protons, were used in the experiment, of which the former were produced from a uranium-plating copper slice while the latter were obtained as a result of neutrons emitting from ^{252}Cf bombarding polythene. The energy of the particles was about several MeV.

The measurement system mainly consisted of an ORTEC B-017-150-300 totally depleted silicon surface barrier detector, an ORTEC 556 high voltage power supply, a Canberra Model 2003BT pre-amplifier, an ORTEC 9302 fast amplifier, and a CAEN v1729A digitizer equipped with a 2GS/s 14 bit ADC. The ORTEC B-017-150-300 totally depleted silicon surface barrier detector, with a thickness of 300 μm and an area of 150 mm^2, was chosen to detect the particles. It has been proven that the current shape of charged particles in solid state detectors is mainly governed by the plasma erosion effect and the charge carrier collection effect [1, 19]. Because the rear side injection amplifies the plasma erosion time differences and the energy thresholds are significantly lower than that in the case of front side injection [1, 2], the detector was mounted in reverse configuration with an applied voltage of 200 V, while the depleted voltage was 72 V. The high voltage was provided by the ORTEC 556 high voltage power supply.

The preamplifier Canberra Model 2003BT provides two outputs, an energy output indicating the energy information and a timing output indicating the current shape of detected particles. Since the current signal is too weak, the timing output should pass through a fast amplifier ORTEC 9302. Then together with the energy output, it was transmitted to the CAEN v1729A digitizer, which is equipped with a 2 GS/s-14 bit ADC.

2.2 Typical pulse waveform

The typical current pulse and charge pulse waveforms of protons and alpha particles with energy of 4.1 MeV are shown in Fig.2. Figure 2(a) shows that there is no obvious difference between the charge pulse waveform of the proton and that of the alpha particle under the same particle energy. However, in Fig. 2(b), the peak value of the proton current pulse is obviously larger than that of the alpha current pulse, which is consistent with the viewpoint given by G. Pausch et al. that the heavier ion generates a current signal of smaller amplitude [7].

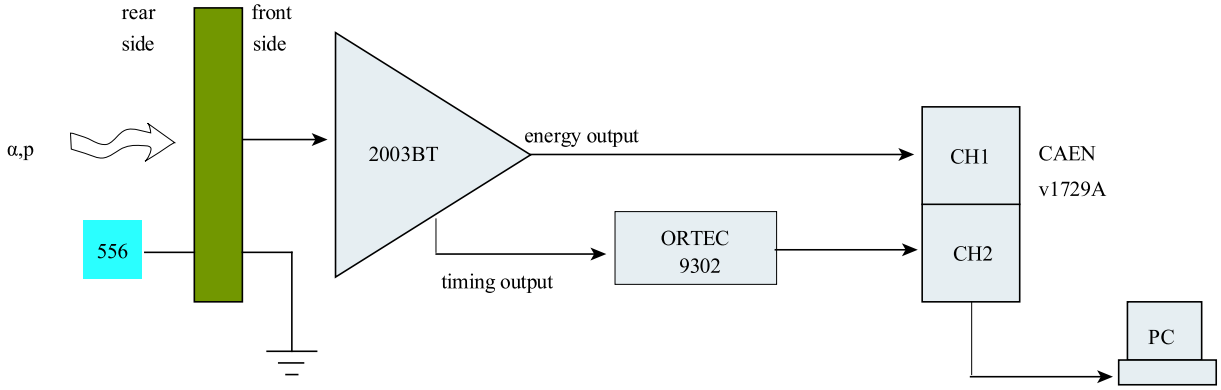

Fig. 1. Schematic of experimental setup.

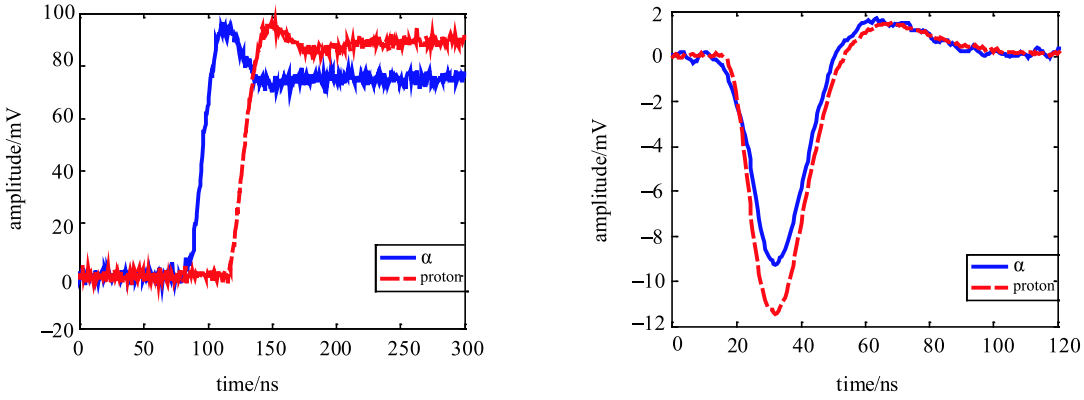

(a) Typical charge pulses of particles (b) Typical current pulses of particles

Fig. 2. (color online) Typical pulse waveform of protons and alpha particles with energy of 4.1 MeV.

2.3 Energy calibration

Calibration needs to be completed in order to get the particles' energy, and the alpha particles were employed to do this. In the uranium used in this experiment, the ^{235}U had been extracted out, leaving ^{238}U and ^{234}U with decay alpha particle' main energies of 4.196 MeV and 4.776 MeV respectively. As shown in Fig. 3, there are two peaks in the ADC spectrum corresponding to the two energy values mentioned above. Because of the linear relationship between the energy and the ADC channel, these two energy points are enough to accomplish the calibration. Figure 4 shows the results.

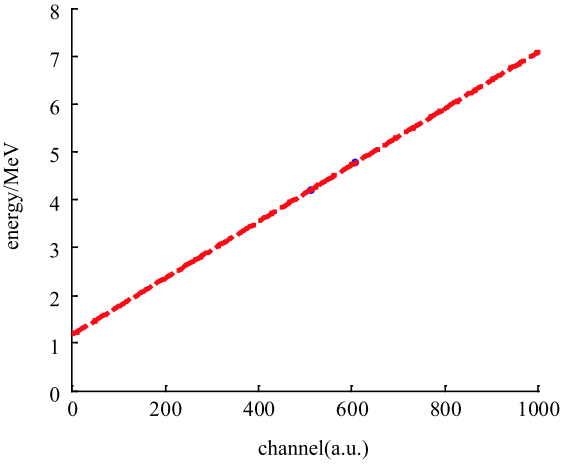

Fig. 4. (color online) Energy calibration of the ADC.

3 Analysis and results

3.1 Frequency Ratio Analysis method

Assuming a digitized pulse signal $x(n)(n=0,1,\cdots,N-1)$, its discrete Fourier transform (DFT) $X(k)$ can be obtained through the following analysis equation [20]

$$X(k)=\sum_{n=0}^{N-1}x(n)\exp\left(-\mathrm{j}\frac{2\pi}{N}nk\right)\quad k=0,1,\cdots,N-1 \quad (1)$$

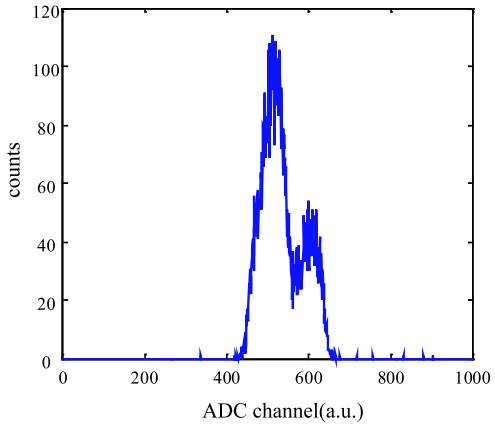

Fig. 3. (color online) Relationship between counts and ADC channel numbers.

where the integer variable n is the discrete time index, N is the sample length, and the integer index k represents the discrete frequency variable corresponding to an actual frequency of kF_s/N, where F_s is the sampling frequency in units of Hz [18]. According to Eq.(1), the magnitude spectrum $|X(k)|$ can be expressed as

$$|X(k)|=\sqrt{\left(\sum_{n=0}^{N-1}x(n)\cos\frac{2\pi nk}{N}\right)^2+\left(\sum_{n=0}^{N-1}x(n)\sin\frac{2\pi nk}{N}\right)^2}. \quad (2)$$

For the current pulse waveforms of proton and alpha particles shown in Fig. 2(b), their magnitude spectra should have an obvious difference due to their different time domain waveforms. Analyzing the frequency magnitude spectrum and looking for the differences between the two particles, we propose a frequency domain method that could catch the significant features to identify protons and alpha particles.

Conducting a discrete Fourier transform (DFT) on the current signals shown in Fig. 2(b), the frequency

spectra of protons and alpha particles were obtained respectively. There are 256 frequency sampling points in all, but at higher frequency, the magnitude is nearly zero, so only some lower frequency components of DFT are given in Fig. 5. As indicated, the spectra of the proton pulse and alpha pulse both rise to a maximum at a frequency index of 1 in the beginning, and then descend rapidly to almost zero after an index of 8, this feature being the same for these two kinds of particles. But we also find that the magnitude difference of the two spectrum waveforms is obvious at the discrete frequency index 0 (i.e. the zero frequency) and index 1 (i.e. the first frequency), which can be used to identify the protons and alpha particles. From Fig. 5, it can be seen that the first frequency component of the alpha magnitude spectrum is nearly the same as that of the proton while the zero frequency component of the alpha magnitude spectrum is much lower than that of the proton. To amplify this important difference, we use the ratio of the first frequency component to the zero frequency component as the identification parameter, which is defined as

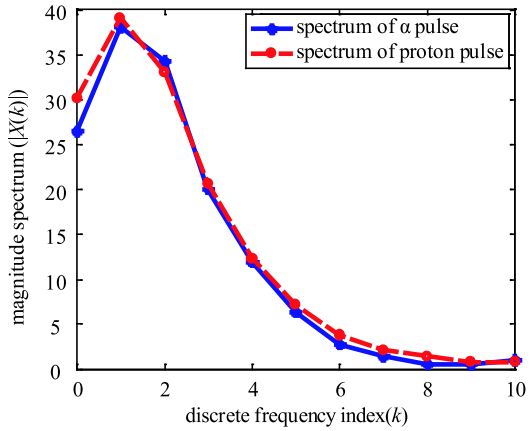

Fig. 5. (color online) Frequency spectrum of the proton and the alpha pulse.

$$d = \frac{|X(1)|}{|X(0)|} \tag{3}$$

where $|X(1)|$ is the first frequency component and $|X(0)|$ is the zero frequency component of the magnitude spectrum respectively. Just as stated above, the difference of $|X(1)|$ between alpha particles and protons is small, while the difference of $|X(0)|$ is much bigger, so the value of d for alpha particles is larger than that for protons, hence accomplishing the identification. According to the identification principle, we name this new method Frequency Ratio Analysis (FRA), and its feasibility and effectiveness are verified with actual experimental data as follows.

3.2 Performance of FRA

A total of 2000 proton events and 2000 alpha events were used to verify the feasibility of the FRA method. The particle energy was calibrated according to the procedures stated in Section 2.3, and the identification parameter is calculated by Eqs.(1)–(3). A scatter plot of d against particle energy is shown in Fig. 6. Clearly, all the particle events are divided into two clusters: one lies in the upper part of the plot, corresponding to the alpha events, while the other lies further down, corresponding to the proton events. At the same time, the identification parameter d decreases with the increasing of energy for both kinds of events. The protons and alpha particles are obviously separated, which proves the feasibility of the FRA method.

To evaluate the separation performance of the FRA method, a figure-of-merit (FOM) is recommended, which is a common measure of the separation defined as [21]

$$\mathrm{FOM} = \frac{S}{\mathrm{FWHM}_1 + \mathrm{FWHM}_2} \tag{4}$$

where S is the separation between the centroids of events peak 1 and events peak 2 in the spectrum, FWHM_1 is the full-width-half-maximum (FWHM) of the spread of events classified as events 1 and FWHM_2 is the FWHM

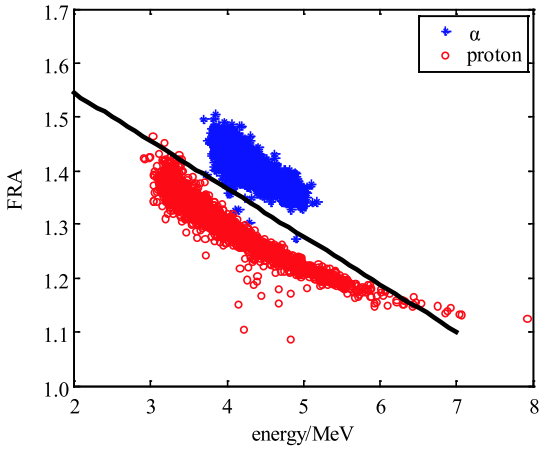

Fig. 6. (color online) Scatter plot of the FRA method.

of the spread of events classified as events 2. The magnitude of FOM reflects the identification performance. Generally speaking, the larger the FOM is, the better the identification performance is. For Gaussian distributions, Eq.(4) can reduce to

$$\mathrm{FOM} = \frac{|\mu_1 - \mu_2|}{2.35(\sigma_1 + \sigma_2)} \tag{5}$$

where μ_1 and μ_2 are mean values of the two Gaussian fits corresponding to events 1 and events 2 respectively, while σ_1 and σ_2 are standard deviations of the two Gaussian fits. In order to get the value of the FOM, an identification line should be plotted in the middle of these two clusters as shown in Fig. 6, and then the probability

distribution against the distance of each point from the identification line is obtained (Fig. 7). It is obvious that there are two peaks, the left one corresponding to the proton events and the right one corresponding to the alpha events. In Fig. 7, the spread of the proton and alpha events are both consistent with a Gaussian distribution. The sum of Gaussian distributions is expressed as

$$f(x) = A_1 \exp\left[-\frac{(x-\mu_1)^2}{2\sigma_1^2}\right] + A_2 \exp\left[-\frac{(x-\mu_2)^2}{2\sigma_2^2}\right] \quad (6)$$

where μ_1, μ_2, σ_1 and σ_2 are the same as those in Eq.(5), whileA_1, A_2 are the scale factor for events 1 and events 2 respectively. With the curve fitting tool in MATLAB software, the probability distribution was Gaussian fitted as the solid line indicates. Table 1 presents the means and standard deviations with uncertainties for the Gaussian fits shown in Fig. 7.

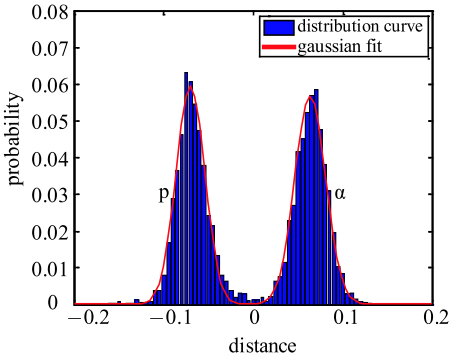

Fig. 7. (color online) Probability distribution histograms with fitted Gaussian distributions for the FRA method.

As listed in Table 1, the FOM of the FRA method is 1.7148, much larger than 1, proving that the FRA method is feasible. In addition, the proton and alpha peaks in Fig. 7 are well separated visually. In summary, the feasibility and effectiveness of the FRA method are verified with a good identification performance.

3.3 Comparison with other methods

The FRA method does well in the identification of the protons and alpha particles by fully taking advantage of the particle information through digital signal processing, moving forward a step with the Fourier transform to analyze the frequency properties of the acquired pulse waveform.

For further understanding of the FRA method, it is essential to compare it with time domain methods. For this reason, two methods, the current pulse amplitude method [7] and the second moment method [14], of which the identification parameter were the maximum amplitude of the current pulse and the second moment m_2 of the current pulse respectively, were chosen to be compared with the FRA method. With similar steps, the scatter plots of these two time domain methods were obtained as shown in Fig. 8, while the probability distribution plots are shown in Fig. 9. Table 2 presents the means and standard deviations with uncertainties for the Gaussian fits shown in Fig. 9.

As listed in Table 2, the FOM of the current pulse amplitude method is 1.1864, and the FOM of the second moment method is 1.3794. For these results, the FOM of the FRA method is about 45 and 24 percent larger than that of the current pulse amplitude method and the second moment method respectively, which indicates a better identification performance of the FRA method than the other two methods. Once the frequency domain method is applied, it achieves quite a large improvement in performance over traditional time domain methods.

Table 1. Values of parameters in Eq.(6) for the FRA method.

μ_1	σ_1	μ_2	σ_2	FOM
−0.0699±0.0005	0.0161±0.0005	0.0651±0.0005	0.0174±0.0005	1.7148±0.0363

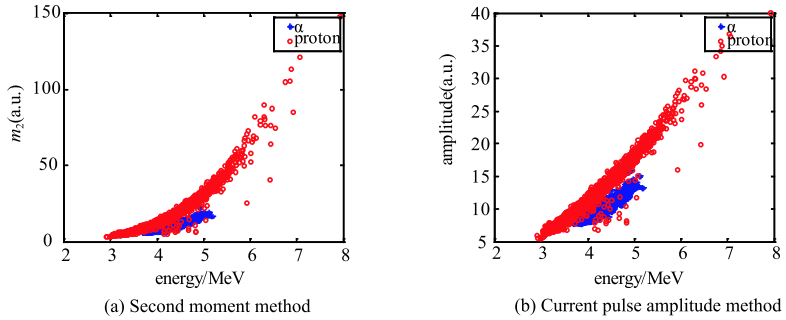

Fig. 8. (color online) Scatter plots of the two time domain methods.

Table 2. The values of parameters in Eq. (6) for two time domain methods.

method	μ_1	σ_1	μ_2	σ_2	FOM
the current pulse amplitude method	−0.2134±0.0057	0.0809±0.0057	0.2357±0.0064	0.0802±0.0064	1.1864±0.0670
the second moment method	−0.2324±0.0027	0.0607±0.0028	0.2414±0.0062	0.0855±0.0062	1.3794±0.0671

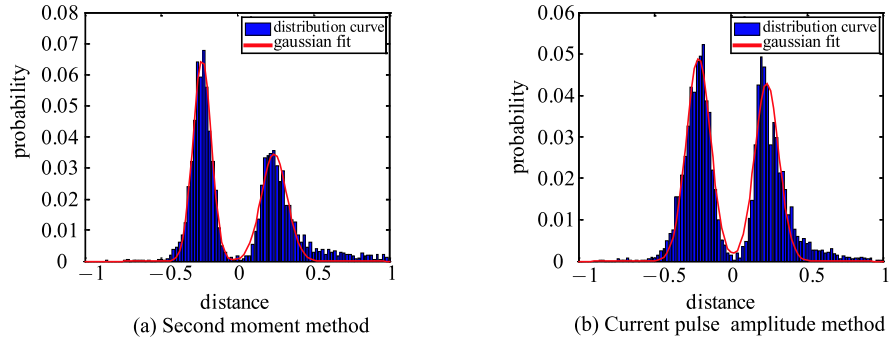

Fig. 9. (color online) Probability distribution histograms with fitted Gaussian distributions for the two time domain methods.

4 Conclusions

In this paper, frequency analysis was introduced into charged particle identification. The signals of the protons and alpha particles were acquired from an experimental system. Through analysis of the signals, a new method called Frequency Ratio Analysis (FRA) was proposed, of which the performance was evaluated and compared with the current pulse amplitude method and the second moment method.

The results showed that the FRA method is not only feasible and effective but also superior to these two time domain methods. It achieves a nearly 45% increase in value of FOM compared with the current pulse amplitude method, and for the second moment method, a 24% increase, which clearly demonstrates the advantage of the frequency method. Since the FRA method just uses the zero-frequency component $|X(0)|$ and the first frequency component $|X(1)|$, while the noise is mainly concentrated in the high frequency components, the FRA method has good noise resistance. Besides, the calculation work is acceptable for only computing $|X(0)|$and $|X(1)|$, making it possible for real-time processing. In future work, we will generalize the FRA method to identify all the heavy charged particles rather than just protons and alpha particles, by doing experiments with a heavy ion accelerator.

References

1 S. Barlini, R. Bougault, Ph. Laborie et al, Nucl. Instrum. Methods A, **600**(3): 644–650 (2009)
2 N. LeNeindre, R. Bougault, S. Barlini et al, Nucl. Instrum. Methods A, **701**(1): 145–152 (2013)
3 L. Bardelli, M. Bini, G. Casini et al, Nucl. Instrum. Methods A, **654**(1): 272–278 (2011)
4 S. Carboni, S. Barlini, L. Bardelli et al, Nucl. Instrum. Methods A, **664**(1): 251–263 (2012)
5 W. Seibt, K. E. Sundstrom, and P. A. Tove, Nucl. Instrum. Methods, **113**(3): 317–324 (1973)
6 A. Alberigi, M. Martini, and G. Ottaviani, IEEE Trans. Nucl. Sci, **16**(2): 35–61 (1969)
7 G. Pausch, H. G. Ortlepp, W. Bohne et al, IEEE Trans. Nucl. Sci, **43**(3): 1097–1101 (1996)
8 C. A. J. Ammerlaan, R .F . Rumphorst, and L .A .CH. Koerts, Nucl. Instr. and Meth., **22**(1): 189–200 (1963)
9 W. D. Emmerich, K. Frank, A. Hofmann et al, Nucl. Instrum. Methods, **83**(1): 131–132 (1970)
10 G. Pausch, W. Bohne, H. Fuchs et al, Nucl. Instrum. Methods A, **322**(1): 43–52 (1992)
11 G. Pausch, W. Bohne, D. Hilscher, Nucl. Instrum. Methods A, **337**(2–3): 573–587 (1994)
12 G. Pausch, W. Bohne, D. Hilscher et al, Nucl. Instrum. Methods A, **349**(1): 281–288 (1994)
13 G. Pausch, M. Moszynski, D. Wolski et al, Nucl. Instrum. Methods A, **365**(1): 176–184 (1995)
14 H. Hamrita, E. Rauly, Y. Blumenfeld et al, Nucl. Instrum. Methods A, **531**(3): 607–615 (2004)
15 G. Liu, M. J. Joyce, X. Ma et al, IEEE Trans. Nucl. Sci, **57**(3): 1682–1691 (2010)
16 Jun Yang, X. L. Luo, G. Liu et al, Chin. Phys. C, **36**(6): 544–551 (2012)
17 G. Liu, X. L. Luo, J. Yang et al, Chin. Phys. C, **37**(6): 201–207 (2013)
18 G. Liu, J. Yang, X. L. Luo et al, Rad. Meas., **58**(5): 12–17 (2013)
19 J. B. A. England, G. M. Field, and T. R. Ophel, Nucl. Instrum. Methods A, **280**(2-3): 291–298 (1989)
20 A. V. Oppenheim, R. W. Schafer, and J. R. Buck, *Discrete-time Signal Processing*, (Second edition, Upper Saddle River, New Jersey: Prentice-Hall, Inc., 1999), p. 561
21 R. A. Winyard, G. W. McBeth, Nucl. Instrum. Methods, **95**(1): 141–153 (1971)